Forensic Science International 353 (2023) 111878

Contents lists available at ScienceDirect

Forensic Science International

journal homepage: www.elsevier.com/locate/forsciint

Diagnostic accuracy of coronary artery stenosis and thrombosis assessment using unenhanced multiplanar 3D post-mortem cardiac magnetic resonance imaging

Paolo Lombardo [a,b], Nicolas Lange-Herr [a], Hanno Hoppe [c,d,e], Nicole Schwendener [a], Christian Jackowski [a], Jeremias Klaus [a,b], Wolf-Dieter Zech [a,*]

[a] Institute of Forensic Medicine, University of Bern, Bern, Switzerland
[b] Department of Diagnostic, Interventional and Pediatric Radiology, Inselspital, Bern University Hospital, University of Bern, Bern, Switzerland
[c] Department of Radiology, Lindenhofspital Bern, Bern, Switzerland
[d] University of Bern, Bern, Switzerland
[e] Department of Health Sciences and Medicine, University of Lucerne, Lucerne, Switzerland

ARTICLE INFO

Keywords:
PMCMR
Coronary artery stenosis
3D sequence
Multiplanar image analysis

ABSTRACT

Background: A 3D sequence was introduced to unenhanced post-mortem cardiac magnetic resonance imaging (PMCMR) to enable multiplanar coronary artery image analysis and to investigate its diagnostic accuracy for the diagnosis of coronary artery stenosis and thrombosis.

Materials and Methods: N = 200 forensic cases with suspected coronary artery pathology underwent 3 Tesla PMCMR (sequence used: T2 weighted transversal 3D turbo spin echo) before autopsy. Main coronary artery stenosis and thrombosis were assessed in PMCMR by multiplanar image analysis by two observers. Coronary artery histology was determined as the gold standard and compared to PMCMR. Sensitivity, specificity, negative (NPV) and positive predictive values (PPV) with 95% confidence intervals were calculated.

Results: For all coronary arteries combined, sensitivity was 75% (PPV 73%) for the diagnosis of stenosis and 72% (PPV 71%) for the diagnosis of thrombosis. Specificity was 92% (NPV 90%) for correct diagnosis of non-existing stenosis and 97% (NPV 97%) for non-existing thrombosis. Sensitivity for correct diagnosis of different degrees of stenosis ranged between 67% and 80% (PPVs 67–82%); specificity ranged between 96% and 99% (NPVs 96–99%).

Conclusion: Multiplanar PMCMR coronary artery stenosis and thrombosis assessment based on an unenhanced T2 weighted 3D sequence provide moderate sensitivity and high specificity for the diagnosis of coronary artery stenosis and/or thrombosis. Hence, 3D T2w PMCMR cannot reliably detect existing coronary artery stenosis and thrombosis but may be particularly useful for the exclusion of stenosis or thrombosis of the main coronary arteries.

1. Introduction

Post-mortem cardiac magnetic resonance imaging (PMCMR) is a core subspecialty in post-mortem imaging [1–6]. Previous studies demonstrated that PMCMR is particularly suitable for the diagnosis of myocardial infarction [7–12]. Even though most cases of myocardial infarction are related to coronary artery stenosis or thrombosis [13], there is a lack of systematic research on these particular coronary pathologies in PMCMR. Coronary artery stenosis is most commonly caused by coronary artery disease (CAD) causing atherosclerotic plaque buildup in the artery wall and narrowing of the vessel lumen [13]. Coronary artery thrombosis is defined as the formation of a blood clot inside the coronary vessel most commonly caused as a downstream effect of coronary atherosclerosis [13,14]. In post-mortem MRI case studies the cross-sectional appearance of vital thrombosis is described as a homogeneous vessel occluding structure of intermediate signal intensity in T2-weighted images [15–17]. Currently, there is no systematic research that investigated coronary artery thrombosis diagnosis in post-mortem MRI. As for coronary artery stenosis, there is only one systematic post-mortem in situ MR study by Ruder et al. who investigated coronary

* Correspondence to: University of Bern, Institute of Forensic Medicine Bern, Murtenstrasse 26, Bern 3008, Switzerland.
E-mail address: Wolf-Dieter.Zech@irm.unibe.ch (W.-D. Zech).

https://doi.org/10.1016/j.forsciint.2023.111878
Received 23 June 2023; Accepted 18 October 2023
Available online 5 November 2023
0379-0738/© 2023 The Authors. Published by Elsevier B.V. This is an open access article under the CC BY license (http://creativecommons.org/licenses/by/4.0/).

artery stenosis in PMCMR in the year 2014 [18]. In their study, Ruder et al. evaluated coronary arteries using unenhanced conventional 1.5 Tesla PMCMR T2 weighted images and compared it to findings of coronary artery stenosis on autopsy. Their study demonstrated, that the occurrence of coronary artery chemical shift artifacts rather indicates vessel patency while the appearance of paired dark bands rather indicates relevant stenosis [18]. However, a direct assessment of coronary artery stenosis in PMCMR was not possible at that time due to a rather low signal-to-noise ratio at 1.5 Tesla and fixed cardiac MRI image planes.

In general, the radiological judgment of the coronary arteries in cross-sectional images is optimal if the vessel lumen can be viewed in longitudinal and transverse image planes along the whole course of the artery [19–22]. Conventional PMCMR uses sequences that produce cardiac images in fixed image planes. The most common PMCMR image planes are the short-axis view, four-chamber view, and two-chamber view [1,5,18]. While these image planes are well suited for the evaluation of myocardium, cardiac cavities, and valves, they are less suited for coronary artery evaluation. Hence, due to the variable tortuous anatomic courses of coronary arteries, their entire course cannot be assessed in orthogonal transverse or longitudinal planes. For optimal PMCMR coronary artery thrombosis and stenosis analysis, a multiplanar approach is recommended. However, two-dimensional datasets generated with conventional PMCMR sequences do not allow for multiplanar image reconstruction. A potential solution to overcome this problem is provided by 3D MRI sequences. Such sequences enable rapid imaging of larger tissue volumes with high spatial resolution resulting in very thin image layers without loss of image quality and a high signal-to-noise ratio. 3D MRI sequences can produce the same image weightings as conventional 2D sequences (such as T1w and T2w) and allow for a multiplanar coronary artery image reconstruction using dedicated software [23–27]. Due to the relatively small caliber of the coronary arteries, a higher signal-to-noise ratio is mandatory. Thus, 3 Tesla field strength is preferred over 1.5 Tesla due to its improved signal-to-noise ratio.

So far, a 3D MRI sequence has not been systematically used for a PMCMR application. We hypothesize that unenhanced multiplanar 3 Tesla coronary artery image analysis based on a 3D sequence is feasible for the diagnosis of coronary artery stenosis and thrombosis in PMCMR. Therefore, the goal of the present study was to evaluate the diagnostic accuracy of multiplanar coronary artery stenosis and thrombosis assessment in unenhanced 3D PMCMR compared to autopsy and histology.

2. Methods and Materials

2.1. Study design and subjects

This prospective study was conducted between 2017 and 2022. Study subjects were n = 200 forensic cases (n = 110 males, n = 90 females, median age of all gender 53 years) investigated at the author's forensic institution. Autopsies were ordered by the local prosecutors. Inclusion criteria were age over 18 years and known coronary artery disease (according to medical reports) or coronary artery calcifications diagnosed on post-mortem computed tomography (PMCT) that was routinely performed in each case before PMCMR. Exclusion criteria were counter to the latter as well as cases with putrefaction gas or metallic coronary artery stents as observed in PMCT.

2.2. Technical PMCMR parameters

Study subjects underwent 3 Tesla PMCMR before autopsy. Bodies were wrapped in a linen sheet and placed on the MRI table in a supine position. The sequence used was a T2 weighted transversal 3D turbo spin echo sequence (PHILIPS, scan parameters: field of view (FoV): 180 mm, slices: 175, thickness: 0.7 mm, repetition time (TR): 1500 ms, echo time (TE): 248 ms, number of signal averages (NSA): 2). The 3D sequence lasted between 15 and 20 min. Post-mortem interval (time between death and MRI scan) ranged between 1 and 3 days (mean 1.8 days).

2.3. PMCMR multiplanar image analysis

Out of 200 cases, 800 single main coronary arteries (comprising left main coronary artery (LMCA), left anterior descending artery (LAD), circumflex artery (CX), and right coronary artery (RCA) were evaluated for coronary artery stenosis and coronary artery thrombosis. A thickening of the vessel wall with consecutive narrowing of the vessel lumen was determined as stenosis. Focal intraluminal structures of intermediate signal intensity in T2-weighted images of the investigated coronary arteries were determined as thrombosis according to Jackowski et al. [15–17].

Two observers (a board-certified radiologist with 7 years of experience in post-mortem imaging and a board-certified forensic pathologist with 12 years of experience in post-mortem imaging) analyzed coronary artery PMCMR images independently and blinded to autopsy and histology results. In cases of disagreements, a consensus was reached in subsequent readings. Images were viewed in a PACS (Sectra Workstation IDS7, Version 20.2.8.3353, 2018, Sectra AB, Linköping) using the built-in multiplanar image reconstruction (MPR) tool. Image planes were adapted manually to gain optimal transverse and longitudinal views of coronary arteries over the whole course of the vessel (Fig. 1). The following parameters were assessed:

1. Existence of stenosis (Fig. 2) independent of the degree of stenosis; location of stenosis (at the proximal, intermediate, or distal portion of the vessel), degree of stenosis according to the SCCT grading scale for stenosis severity (0% no stenosis; 1–24% minimal stenosis, 25–49% mild stenosis; 50–69% moderate stenosis; 70–99% severe stenosis; 100% occluded) [28].
2. Existence of thrombosis (Fig. 3); location of thrombosis (at the proximal, intermediate, or distal portion of the vessel).

2.4. Cardiac autopsy dissection and histology

Board-certified forensic pathologists performed cardiac dissection at forensic autopsy. This included opening all main coronary arteries by multiple transverse cuts of about 3 mm intervals along the whole course of the vessels. The existence and location (at the proximal, intermediate, or distal portion of the coronary artery vessel) of stenosis and/or thrombosis were noted in the autopsy protocol. Coronary artery sections with stenosis and/or thrombosis were removed and processed for histologic examinations (hematoxylin and eosin (HE) stain) as part of routine post-mortem examinations. The degree of coronary artery stenosis was assessed as a percentage at histologic slides based on decalcified HE stains by a forensic pathologist (with over 10 years of experience in the field of cardiovascular pathology) blinded to imaging results. The existence of coronary artery thrombosis was confirmed histologically. Differentiation between vital thrombosis and post-mortem clotting was determined at histologic slides according to Dettmeyer et al. [29].

2.5. Statistical analysis

Autopsy/histology coronary artery stenosis and thrombosis findings were compared to PMCMR findings. The following parameters were compared: the existence of stenosis (independent of the degree of stenosis), location of stenosis (at the proximal, intermediate, or distal portion of the vessel), degree of stenosis (as a percentage), the existence of thrombosis, location of thrombosis (at the proximal, intermediate or distal portion of the vessel). For LMCA, the location of stenosis or thrombosis was not determined due to its short anatomical vessel course. The histology of main coronary artery findings was determined

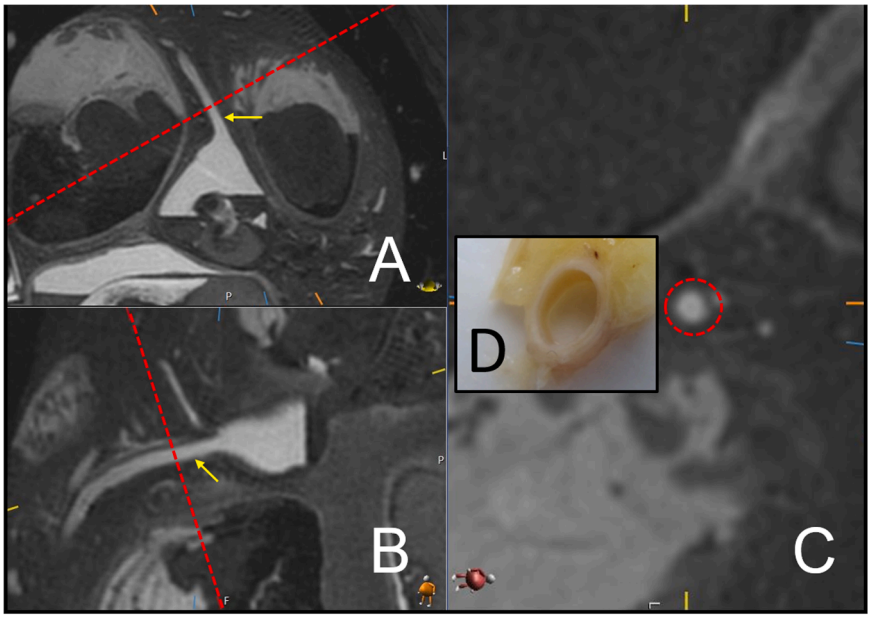

Fig. 1. 3D based multiplanar unenhanced PMCMR T2w images of the right coronary artery (RCA, yellow arrows) shortly after its aortic origin with no findings. Manual adjustment of the different plane axes (artificial added dashed red lines in A and B) enables optimal longitudinal and transversal (dashed red circle in C and autopsy finding in D) image plane views of the vessel lumen over the whole course of the vessel.

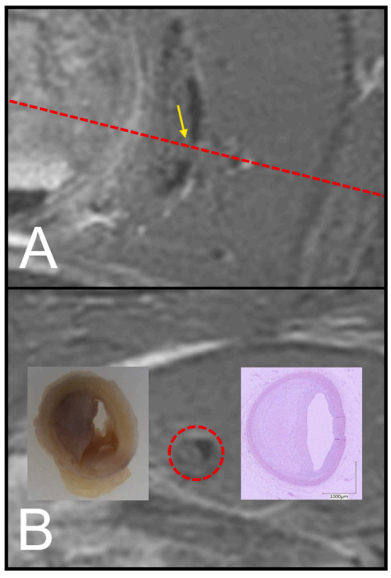

Fig. 2. 3D-based multiplanar unenhanced PMCMR T2w images of the right coronary artery (RCA, yellow arrows) at its intermediate section. Manual adjustment of the image plane (artificial dashed red line in A) enables an optimal transversal view (B) of the vessel lumen with stenosis (yellow arrow in A, dashed red circle in B with autopsy and histology stenosis findings). Notice that the actual degree of stenosis can be judged in the transversal view in B only.

as the gold standard and compared to PMCMR findings. Sensitivity, specificity, and negative and positive predictive values with 95% confidence intervals (CI) were calculated according to the following parameters: True positive: consistent diagnosis of localization and existence of stenosis or thrombosis. True negative: consistent diagnosis of non-existing stenosis or thrombosis. False positive: localization and existence of stenosis or thrombosis diagnosed in PMCMR but not at autopsy/histology. False negative: stenosis or thrombosis diagnosed at autopsy/histology but not at PMCMR. As for degrees of stenosis, the

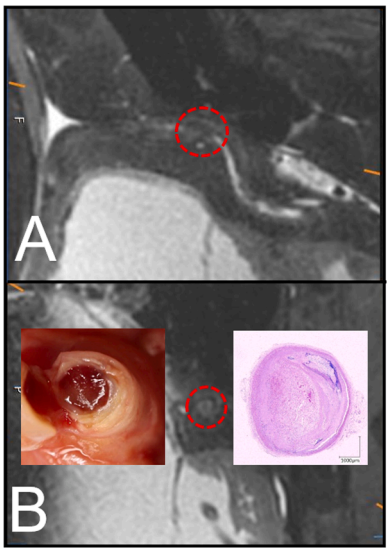

Fig. 3. 3D based multiplanar unenhanced PMCMR T2w images of the right coronary artery (RCA) at its intermediate section showing stenosis and thrombosis with intermediate signal in the longitudinal plane (dashed red circle in A) and the transversal plane (dashed red circle in B with autopsy finding and histology finding).

following parameters were defined: True positive: consistent diagnosis of a particular degree of stenosis. True negative: consistent diagnosis of non-existing stenosis. False positive: particular degree of stenosis diagnosed in imaging but not at autopsy/histology. False negative: particular degree of stenosis diagnosed at autopsy/histology but not at imaging.

PMCMR inter-observer reliability for the existence of stenosis and degree of stenosis as well as the existence of thrombosis was determined by using the weighted kappa statistic as reported by Siegel 1988 [30] and interpreted as follows: excellent agreement: $\kappa > 0.81$; good agreement: $\kappa = 0.61–0.80$; moderate agreement: $\kappa = 0.41–0.60$; slight agreement: $\kappa = 0.21–0.40$; poor agreement: $\kappa = 0–20$. The SPSS® software package (Version 23.0) was used for all calculations.

3. Results

Out of 200 hearts, n = 156 hearts presented with one or more main coronary artery stenosis. N = 35 hearts showed one or more coronary artery thrombosis on autopsy/histology. In n = 29 hearts, both coronary artery stenosis and thrombosis were present. Table 1 demonstrates localizations and total numbers of stenoses, numbers of different degrees of stenoses, and numbers of thromboses diagnosed on autopsy/histology and PMCMR. In total n = 223 coronary artery stenoses and n = 43 thromboses were diagnosed on autopsy/histology and n = 213 stenoses and n = 45 thromboses were diagnosed using PMCMR. The majority of stenoses (63% histology; 50% PMCMR) and thromboses (51% histology; 53% PMCMR) were observed in the proximal sections of the coronary arteries (including the left main coronary artery) on both autopsy/histology and PMCMR. Least stenoses (9% histology, 8% PMCMR) and thromboses (9% histology, 7% PMCMR) were observed in the distal coronary sections. Out of n = 43 thromboses seen at autopsy, n = 4 thromboses were diagnosed as post-mortem clots in histology. In PMCMR, these clots appeared with intermediate signal intensity and were not distinguishable from the signal appearance of vital thrombosis.

Table 2 demonstrates sensitivity, specificity, and positive and negative predictive values for comparison between autopsy/histology and PMCMR. For all coronary arteries combined, sensitivity for the diagnosis of stenosis was 75% (PPV 73%). Specificity was 92% for correct diagnosis of non-existing stenosis (NPV 92%). Sensitivity for correct diagnosis of different degrees of stenosis ranged between 67% and 80% (PPVs 67–82%); specificity ranged between 96% and 99% (NPVs 96–99%). For all coronary arteries combined, sensitivity for the diagnosis of thrombosis was 72% (PPV 71%). Specificity was 97% (NPV 97%) for the correct diagnosis of non-existing thrombosis.

Inter-observer agreement was excellent for the diagnosis of non-existing stenosis (κ-value 0.91) and non-existing thrombosis (κ-value 0.85). Good agreement was observed for the diagnosis of stenosis independent of the degree of stenosis (κ-value 0.77), stenosis 1–24% (κ-value 0.79), stenosis 25–49% (κ-value 0.75), stenosis 50–69% (κ-value 0.70), stenosis 70–99% (κ-value 0.77), stenosis 100% (κ-value 0.71) and thrombosis (κ-value 0.74).

Time effort per observer for evaluation of the coronary arteries off one single heart at PMCMR was approximately 5 min for hearts without coronary artery pathology and approximately 10–15 min for hearts with coronary artery pathology.

4. Discussion

The present study demonstrates moderate sensitivity and high specificity for the diagnosis of main coronary artery stenosis and thrombosis based on an unenhanced 3D T2 weighted PMCMR sequence. The results show that the multiplanar 3D PMCMR approach cannot reliably detect existing coronary artery stenosis and thrombosis. However, high specificity and negative predictive values indicate that the method may be particularly useful for the exclusion of stenosis or thrombosis. So far, PMCMR mainly focused on the judgment of the myocardium [6]. Coronary artery evaluation was neglected because conventional unenhanced PMCMR imaging is rather unsuitable for coronary artery assessment [18]. The 3D multiplanar approach provides a tool to narrow the existing gap between myocardial and coronary PMCMR evaluation. Conventional PMCMR can adequately visualize both acute and chronic myocardial damage. For instance, myocardial infarction older than a few hours causes myocardial signal alterations depending on the used MR image weightings [7–12]. Hence, combined findings of missing myocardial signal alterations in conventional PMCMR and missing hints of relevant coronary artery stenosis and/or thrombosis in the multiplanar coronary evaluation indicate the absence of acute myocardial infarction aged older than a few hours. If PMCMR myocardial signal alterations indicate acute or older myocardial damage, multiplanar coronary artery analysis can aid in identifying coronary artery culprit lesions but it cannot safely confirm them.

Only moderate sensitivities for coronary artery stenosis and thrombosis may be explained by varying PMCMR T2w signal appearances of arteriosclerotic vessel wall changes on the one hand and varying signal appearances of blood within the coronary vessel lumen on the other hand. Previous clinical and ex-vivo MRI studies demonstrated that arteriosclerotic vessel wall changes might appear with various signal intensities in T2w [31–34]. On post-mortem MRI (PMMR) it is known that blood can appear sedimented or non-sedimented. In T2w PMMR images, sedimented blood appears with a hyperintense upper serum layer and a hypointense lower cellular layer. Non-sedimented blood rather appears hyperintense on T2w images but may also appear with intermediate signal intensity depending on blood composition and blood clotting in particular [15]. It can be hypothesized, that if coronary artery stenosis in post-mortem T2w appears with signals similar to blood it may be hard or impossible to detect. The same phenomena might account for coronary artery thrombosis. By previous literature, all of the investigated coronary artery thromboses in this study appeared with intermediate signals in T2w [15–17]. If coronary artery vessel wall and thrombosis both show intermediate signals, thrombosis may be hard or impossible to detect. Varying signal intensities of the coronary artery vessel wall and blood components may also cause stenosis to be misinterpreted as thrombosis and vice versa. Moreover, the present study showed that T2w PMCMR could not reliably differentiate between vital

Table 1
Numbers of coronary artery stenosis and thrombosis diagnosed at autopsy/histology and PMCMR. Numbers are shown for all coronaries combined as well as for single coronary arteries (LMCA: left main coronary artery; LAD: left anterior descending artery; CX: circumflex artery; RCA: right coronary artery). *LMCA was not included because it was not divided into different vessel sections due to its short anatomical vessel course.

		All coronary arteries		LMCA		LAD		CX		RCA	
		Autopsy	PMCMR	Autopsy	PMCMR	Autopsy	PMCMR	Autopsy	PMCMR	Autopsy	PMCMR
No Stenosis		577	587	169	167	124	129	152	152	132	138
Stenosis all degrees		223	213	31	33	76	71	48	48	68	62
Localization Stenosis*	*proximal*	110	107	na	na	42	40	27	30	41	38
	inter- mediate	62	56	na	na	25	23	15	13	22	20
	distal	20	17	na	na	9	8	6	5	5	4
Degree Stenosis	1–24%	46	44	7	6	13	13	10	9	16	15
	25–49%	50	47	6	6	19	15	10	11	15	14
	50–69%	55	52	7	9	19	17	12	13	16	15
	70–99%	56	57	7	9	20	22	12	11	18	16
	100%	16	13	4	3	5	4	4	4	3	2
No Thrombosis		757	755	193	188	184	183	191	189	188	189
Thrombosis		43	45	7	12	16	17	9	11	12	11
Localization Thrombosis*	*proximal*	22	24	na	na	10	11	7	8	6	5
	inter- mediate	17	18	na	na	4	4	2	3	4	4
	distal	4	3	na	na	2	2	0	0	2	2

Table 2
Sensitivity, Specificity, negative (NPV) and positive (PPV) predictive values with 95% confidence intervals (CI) for coronary artery stenosis and thrombosis comparison of autopsy and PMCMR.

	Sensitivity % (CI %)	PPV % (CI %)	Specificity % (CI %)	NPV % (CI %)
LMCA				
	76 (57–86)	74 (57–83)	95 (90–97)	95 (92–97)
1–24%	80 (53–90)	82 (53–94)	99 (95–99)	97 (96–99)
25–49%	78 (57–98)	73 (46–89)	98 (96–99)	99 (97–99)
50–69%	75 (49–93)	76 (42–76)	98 (94–99)	99 (96–99)
70–99%	74 (50–89)	68 (41–88)	99 (94–99)	98 (95–99)
100%	77 (59–87)	72 (44–87)	98 (94–99)	98 (95–99)
Thrombosis	72 (51–88)	70 (45–81)	97 (93–99)	98 (96–99)
LAD				
Stenosis all degress	75 (69–87)	74 (75–91)	92 (85–95)	90 (87–96)
Stenosis 1–24%	73 (54–86)	75 (61–90)	97 (94–99)	96 (93–98)
Stenosis 25–49%	71 (53–85)	77 (68–95)	98 (95–99)	95 (92–97)
Stenosis 50–69%	74 (54–88)	70 (63–90)	96 (92–98)	97 (93–98)
Stenosis 70–99%	77 (55–89)	71 (62–89)	96 (91–98)	98 (92–98)
Stenosis 100%	78 (60–88)	79 (61–88)	97 (90–99)	96 (91–98)
Thrombosis	71 (49–82)	70 (49–79)	96 (92–98)	97 (94–98)
CX				
Stenosis all degrees	75 (61–85)	72 (63–84)	92 (87–95)	92 (88–95)
Stenosis 1–24%	78 (55–91)	77 (56–90)	97 (93–99)	97 (93–99)
Stenosis 25–49%	75 (51–90)	71 (49–86)	96 (92–98)	97 (93–99)
Stenosis 50–69%	72 (53–90)	69 (39–80)	97 (94–99)	97 (96–99)
Stenosis 70–99%	74 (48–88)	67 (42–79)	97 (93–99)	98 (95–99)
Stenosis 100%	74 (49–89)	75 (47–85)	98 (94–99)	98 (94–99)
Thrombosis	70 (50–86)	72 (47–68)	97 (93–99)	98 (96–99)
RCA				
Stenosis all degrees	72 (59–80)	74 (67–85)	90 (83–94)	89 (82–94)
Stenosis 1–24%	67 (48–81)	75 (57–87)	97 (93–99)	95 (92–97)
Stenosis 25–49%	74 (55–87)	81 (61–92)	98 (94–99)	97 (94–98)
Stenosis 50–69%	73 (55–84)	71 (44–81)	97 (93–99)	97 (95–99)
Stenosis 70–99%	73 (44–83)	69 (42–84)	98 (94–99)	98 (94–99)
Stenosis 100%	75 (53–89)	72 (48–88)	98 (94–99)	99 (92–99)
Thrombosis	73 (45–87)	70 (47–84)	98 (95–99)	97 (95–99)
All Coronaries				
Stenosis all degrees	75 (65–81)	73 (70–80)	92 (90–97)	92 (87–95)
Stenosis 1–24%	75 (59–81)	77 (55–86)	98 (92–99)	96 (92–98)
Stenosis 25–49%	75 (61–82)	76 (60–83)	98 (91–99)	97 (90–99)
Stenosis 50–69%	74 (60–85)	72 (59–80)	97 (91–99)	98 (93–99)
Stenosis 70–99%	75 (62–84)	69 (49–79)	97 (92–99)	98 (91–99)
Stenosis 100%	76 (58–84)	75 (55–86)	98 (90–99)	98 (92–99)
Thrombosis	72 (49–81)	71 (45–79)	97 (90–98)	97 (91–99)

thrombosis and post-mortem clotting. It can be hypothesized that adding 3D sequences with additional image weightings, such as T1, may aid in better discrimination between blood components and arteriosclerotic vessel wall changes and thus result in higher diagnostic accuracy for unenhanced PMCMR stenosis and thrombosis evaluation. Further studies are needed to investigate this hypothesis.

So far, no systematic direct assessment of coronary artery stenosis has been done in PMCMR. However, the statistical results of the present study appear similar to the work of Ruder et al. who also found high specificity and lower sensitivity for an indirect PMCMR diagnosis of coronary artery stenosis [18]. Ruder et al. did not directly assess coronary artery stenosis in PMCMR. They evaluated the presence of coronary artery chemical shift artifacts as a marker for significant coronary artery stenosis and the presence of coronary artery paired dark bands as a marker for vessel patency. In the present study, paired dark bands and chemical shift artifacts were observed only occasionally leading to the conclusion that these phenomena cannot reliably be used for PMCMR stenosis evaluation.

In living patients, cardiac magnetic resonance imaging (CMR) is the established gold standard for the noninvasive volumetric and functional assessment of the ventricles, the assessment of myocardial viability, and tissue characterization. However, CMR is not being used routinely for direct assessment of coronary artery disease (CAD) [35–37]. Invasive x-ray-based coronary angiography remains the gold-standard method for the identification and characterization of coronary artery stenosis [38,39]. The current gold standard for coronary artery stenosis evaluation in post-mortem imaging is computed tomography angiography (PMCTA) [40–44]. PMCTA is feasible for visualizing relevant coronary stenosis. However, similar to the results of our study previous PMCTA studies demonstrated moderate sensitivity and high specificity in the diagnosis of coronary artery stenosis [40,41,43]. If the diagnostic accuracy of multiplanar coronary PMCMR does not differ significantly from PMCTA, PMCMR may be considered an alternative to coronary artery PMCTA. Future studies need to evaluate how the results of unenhanced multiplanar coronary artery PMCMR compare to PMCTA.

4.1. Limitations

Although the 3 Tesla approach offers a relatively high image resolution that is sufficient for stenosis judgment of the main coronary arteries, smaller coronary branches such as the left marginal arteries and diagonal branches or right marginal branches are often too small for a sufficient diagnosis of stenosis or thrombosis. PMCMR observers need to be aware that relevant coronary artery stenosis may also occur in smaller coronary branches. Hence, if the main coronary arteries do not exhibit pathological findings, relevant stenosis of smaller branches cannot be excluded in 3D coronary PMCMR per se.

The present study was performed without the use of a contrast agent. Currently, PMCMR coronary artery evaluation is always done unenhanced because coronary artery MR angiography is practically nonexistent in any post-mortem imaging facility worldwide due to high costs, the need for additional dedicated equipment, and relatively long examination times [45–48].

Same as clinical MRI, PMMR is limited by artifacts that may be caused by ferromagnetic objects or gas. In PMCMR, such artifacts may be caused by coronary artery stents, implanted cardiac devices, or putrefaction gas within the coronary artery lumen. The PMCMR observer

has to be aware, that such artifacts may mask coronary artery pathology.

5. Conclusion

Multiplanar PMCMR coronary artery stenosis and thrombosis assessment based on an unenhanced T2 weighted 3D sequence provide moderate sensitivity and high specificity for the diagnosis of main coronary artery stenosis and/or thrombosis. 3D T2w PMCMR cannot reliably detect existing coronary artery stenosis or thrombosis but may be particularly useful for the exclusion of stenosis or thrombosis of the main coronary arteries.

Funding

This research did not receive any specific grant from funding agencies in the public, commercial, or not-for-profit sectors.

Declaration of Competing Interest

The authors declare that they have no known competing financial interests or personal relationships that could have appeared to influence the work reported in this paper.

References

[1] C. Jackowski, W. Schweitzer, M. Thali, K. Yen, E. Aghayev, M. Sonnenschein, P. Vock, R. Dirnhofer, Virtopsy: postmortem imaging of the human heart in situ using MSCT and MRI, Forensic Sci. Int. 149 (1) (2005) 11–23.
[2] C. Jackowski, N. Schwendener, S. Grabherr, A. Persson, Post-mortem cardiac 3-T magnetic resonance imaging: visualization of sudden cardiac death? J. Am. Coll. Cardiol. 62 (7) (2013) 617–629.
[3] G. Ampanozi, P.M. Flach, T.D. Ruder, L. Filograna, W. Schweitzer, M.J. Thali, L. C. Ebert, Differentiation of hemopericardium due to ruptured myocardial infarction or aortic dissection on unenhanced postmortem computed tomography, Forensic Sci. Med. Pathol. 13 (2) (2017) 170–176.
[4] T.D. Ruder, M.J. Thali, G.M. Hatch, Essentials of forensic post-mortem MR imaging in adults, Br. J. Radio. 87 (1036) (2014), 20130567.
[5] G. Ampanozi, G.M. Hatch, P.M. Flach, M.J. Thali, T.D. Ruder, Postmortem magnetic resonance imaging: Reproducing typical autopsy heart measurements, Leg. Med (Tokyo) 17 (6) (2015) 493–498.
[6] G. Femia, N. Langlois, J. Raleigh, S.R. Perumal, C. Semsarian, R. Puranik, Post-mortem cardiac magnetic resonance parameters in normal and diseased conditions, Cardiovasc Diagn. Ther. 11 (2) (2021) 373–382.
[7] C. Jackowski, M. Warntjes, J. Berge, W. Bär, A. Persson, Magnetic resonance imaging goes postmortem: noninvasive detection and assessment of myocardial infarction by postmortem MRI, Eur. Radio. 21 (1) (2011) 70–78.
[8] C. Jackowski, A. Christe, M. Sonnenschein, E. Aghayev, M.J. Thali, Postmortem unenhanced magnetic resonance imaging of myocardial infarction in correlation to histological infarction age characterization, Eur. Heart J. 27 (20) (2006) 2459–2467.
[9] C. Jackowski, M.J. Warntjes, J. Berge, W. Bär, A. Persson, Magnetic resonance imaging goes postmortem: noninvasive detection and assessment of myocardial infarction by postmortem MRI, Eur. Radio. 21 (1) (2011) 70–78.
[10] A. Persson, J. Baeckmann, J. Berge, C. Jackowski, M. Warntjes, W.D. Zech, Temperature-corrected postmortem 3-T MR quantification of histopathological early acute and chronic myocardial infarction: a feasibility study, Int. J. Leg. Med. 132 (2) (2018) 541–549.
[11] N. Schwendener, C. Jackowski, A. Persson, M.J. Warntjes, F. Schuster, F. Riva, W. D. Zech, Detection and differentiation of early acute and following age stages of myocardial infarction with quantitative post-mortem cardiac 1.5T MR, Forensic Sci. Int. 270 (2017) 248–254.
[12] W.D. Zech, N. Schwendener, A. Persson, M.J. Warntjes, C. Jackowski, Postmortem MR quantification of the heart for characterization and differentiation of ischaemic myocardial lesions, Eur. Radiol. 25 (7) (2015) 2067–2073.
[13] R.N. Mitchell, Ischemic Heart disease, in: V. Kumar, A. Abbas, J. Aster (Eds.), Robbins Basic Pathology, ninth ed., Elsevier, Philadelphia, 2013, pp. 274–384.
[14] Adnan G., Singh D.P., Mahajan K. Coronary Artery Thrombus. In: StatPearls [Internet]. Treasure Island (FL): StatPearls Publishing; 2022.
[15] C. Jackowski, M. Thali, E. Aghayev, K. Yen, M. Sonnenschein, K. Zwygart, R. Dirnhofer, P. Vock, Postmortem imaging of blood and its characteristics using MSCT and MRI, Int. J. Leg. Med. 120 (4) (2006) 233–240.
[16] C. Jackowski, S. Grabherr, N. Schwendener, Pulmonary thrombembolism as cause of death on unenhanced postmortem 3T MRI, Eur. Radio. 23 (5) (2013) 1266–1270.
[17] C. Jackowski, K. Hofmann, N. Schwendener, W. Schweitzer, M. Keller-Sutter, Coronary thrombus and peracute myocardial infarction visualized by unenhanced postmortem MRI prior to autopsy, Forensic Sci. Int. 214 (1–3) (2012) e16–e19.
[18] T.D. Ruder, R. Bauer-Kreutz, G. Ampanozi, A.B. Rosskopf, T.M. Pilgrim, O. M. Weber, M.J. Thali, G.M. Hatch, Assessment of coronary artery disease by post-mortem cardiac MR, Eur. J. Radio. 81 (9) (2012) 2208–2214.
[19] S. Sridharan, G. Price, O. Tann, M. Hughes, V. Muthurangu, A.M. Taylor, Imaging planes-coronary arteries. Cardiovascular MRI in Congenital Heart Disease, Springer, Berlin, Heidelberg, 2010.
[20] A. Taylor, J. Bogaert, Cardiovascular MR imaging planes and segmentation, in: J. Bogaert, S. Dymarkowski, A. Taylor (Eds.), Clinical Cardiac MRI, Springer, Berlin, Heidelberg, 2012, pp. 85–97.
[21] K.D. Shelton, Cardiac imaging in acquired diseases, in: W.E. Brant, C.A. Helms (Eds.), Fundamentals of Diagnostic Radiology, third ed., Philadelphia, Lippincott Williams &Wilkins, 2007, pp. 629–651.
[22] D.T. Ginat, M.W. Fong, D.J. Tuttle, et al., Cardiac imaging: Part 1, MR pulse sequences, imaging planes, and basic anatomy, AJR Am. J. Roentgenol. 197 (4) (2011) 808–815.
[23] Y. Tatewaki, T. Mutoh, K. Omodaka, B. Thyreau, I. Matsudaira, H. Furukawa, K. Yamada, K. Kunitoki, R. Kawashima, T. Nakazawa, Y. Taki, Morphological prediction of glaucoma by quantitative analyses of ocular shape and volume using 3-dimensional T2-weighted MR images, Sci. Rep. 9 (1) (2019) 15148.
[24] V.N. Wijayathunga, S.F. Tanner, J.P. Ridgway, R.K. Wilcox, An in vitro study of the intervertebral disc structure using 3 T magnetic resonance imaging, Spine (Philos. Pa 1976) 44 (11) (2019) 793–800.
[25] E. Sartoretti, T. Sartoretti, Á. Schwenk, A. Alfieri, D. Czell, M. Wyss, L. Wildi, C. A. Binkert, S. Sartoretti-Schefer, High-resolution 3D versus standard-resolution 2D T2-weighted turbo spin echo MRI for the assessment of lumbar nerve root compromise, Tomography 8 (1) (2022) 257–266.
[26] B. Sundermann, B. Billebaut, J. Bauer, C.G. Iacoban, O. Alykova, C. Schülke, M. Gerdes, H. Kugel, S. Neduvakkattu, H. Bösenberg, C. Mathys, Practical aspects of novel MRI techniques in neuroradiology: part 1-3D acquisitions, dixon techniques and artefact reduction, Rofo (2022).
[27] K. Matsumoto, H. Yokota, T. Yoda, R. Ebata, H. Mukai, Y. Masuda, T. Uno, Reproducibility between three-dimensional turbo spin-echo and two-dimensional dual inversion recovery turbo spin-echo for coronary vessel wall imaging in Kawasaki disease, Sci. Rep. 12 (1) (2022) 6835.
[28] R.C. Cury, S. Abbara, S. Achenbach, et al., CAD-RADS(TM) coronary artery disease - reporting and data system. an expert consensus document of the society of cardiovascular computed tomography (SCCT), the American College of Radiology (ACR) and the North American Society for Cardiovascular Imaging (NASCI). Endorsed by the American College of Cardiology, J. Cardiovasc Comput. Tomogr. 10 (4) (2016 -) 269–281.
[29] R.B. Dettmeyer, Thrombosis and embolism, in: Forensic Histopathology, Fundamentals and Perspectives, Springer, Berlin Heidelberg, 2011, pp. 173–190.
[30] S.C.N. Siegel, Nonparametric Statistics for the Behavioral Sciences, McGraw-Hill Book Company, New York, 1988 (International Edition).
[31] B. Sun, D.P. Giddens, R. Long Jr, W.R. Taylor, D. Weiss, G. Joseph, D. Vega, J. N. Oshinski, Characterization of coronary atherosclerotic plaque using multicontrast MRI acquired under simulated in vivo conditions, J. Magn. Reson Imaging 24 (4) (2006) 833–841.
[32] M.E. Porambo, J.K. DeMarco, MR imaging of vulnerable carotid plaque, Cardiovasc Diagn. Ther. 10 (4) (2020) 1019–1031.
[33] M. Károlyi, H. Seifarth, G. Liew, C.L. Schlett, P. Maurovich-Horvat, P. Stolzmann, G. Dai, S. Huang, C.J. Goergen, M. Nakano, F. Otsuka, R. Virmani, U. Hoffmann, D. E. Sosnovik, Classification of coronary atherosclerotic plaques ex vivo with T1, T2, and ultrashort echo time CMR, JACC Cardiovasc Imaging 6 (4) (2013) 466–474.
[34] T. Li, X. Li, X. Zhao, W. Zhou, Z. Cai, L. Yang, A. Guo, S. Zhao, Classification of human coronary atherosclerotic plaques using ex vivo high-resolution multicontrast-weighted MRI compared with histopathology, AJR Am. J. Roentgenol. 198 (5) (2012) 1069–1075.
[35] V. Russo, L. Lovato, G. Ligabue, Cardiac MRI: technical basis, Radio. Med. 125 (11) (2020) 1040–1055.
[36] A. Busse, R. Rajagopal, S. Yücel, E. Beller, A. Öner, F. Streckenbach, D. Cantré, H. Ince, M.A. Weber, F.G. Meinel, Cardiac MRI-Update 2020, Radiologe 60 (Suppl 1) (2020) 33–40.
[37] Y. Ge, D.P. Deva, K.A. Connelly, A.T. Yan, Stress cardiac MRI in stable coronary artery disease, Curr. Opin. Cardiol. 35 (5) (2020) 566–573.
[38] A. Mangla, E. Oliveros, K.A.Sr Williams, D.K. Kalra, Cardiac imaging in the diagnosis of coronary artery disease, Curr. Probl. Cardiol. 42 (10) (2017) 316–366.
[39] D.T. Bertolone, E. Gallinoro, G. Esposito, et al., Contemporary management of stable coronary artery disease, High. Blood Press Cardiovasc Prev. 29 (3) (2022) 207–219.
[40] I.S.D. Roberts, R.E. Benamore, C. Peebles, et al., Diagnosis of coronary artery disease using minimally invasive autopsy: evaluation of a novel method of post-mortem coronary CT angiography, Clin. Radio. 66 (2011) 645–650.
[41] G.N. Rutty, B. Morgan, C. Robinson, et al., Diagnostic accuracy of post-mortem CT with targeted coronary angiography versus autopsy for coroner-requested post-mortem investigations: a prospective, masked, comparison study, Lancet 390 (2017) 145–154.
[42] K. Michaud, S. Grabherr, F. Doenz, P. Mangin, Evaluation of post-mortem MDCT and MDCT-angiography for the investigation of sudden cardiac death related to atherosclerotic coronary artery disease, Int. J. Cardiovasc Imaging 28 (2012) 1807–1822.
[43] M.K. Chainchel Singh, S.N. Abdul Rashid, S. Abdul Hamid, M.S. Mahmood, S. S. Feng, H. Mohd Nawawi, E. Omar, Correlation and assessment of coronary artery luminal stenosis: post-mortem computed tomography angiogram versus histopathology, Forensic Sci. Int. 308 (2020), 110171.

[44] S. Grabherr, J. Grimm, P. Baumann, P. Mangin, Application of contrast media in post-mortem imaging (CT and MRI), Radio. Med. 120 (9) (2015) 824–834.
[45] T.D. Ruder, G.M. Hatch, L.C. Ebert, P.M. Flach, S. Ross, G. Ampanozi, M.J. Thali, Whole body postmortem magnetic resonance angiography, J. Forensic Sci. 57 (2012) 778–782.
[46] K. Michaud, S. Grabherr, C. Jackowski, M.D. Bollmann, F. Doenz, P. Mangin, Postmortem imaging of sudden cardiac death, Int. J. Leg. Med. 128 (1) (2014) 127–137.
[47] K. Michaud, P. Genet, S. Sabatasso, S. Grabherr, Postmortem imaging as a complementary tool for the investigation of cardiac death, Forensic Sci. Res 4 (3) (2019) 211–222.
[48] E. De Marco, G. Vacchiano, P. Frati, R. La Russa, A. Santurro, M. Scopetti, G. Guglielmi, V. Fineschi, Evolution of post-mortem coronary imaging: from selective coronary arteriography to post-mortem CT-angiography and beyond, Radio. Med. 123 (5) (2018) 351–358.